# Preparation and Characterisation of Mixed Bismuth and Ruthenium Clusters; *X*-Ray Crystal Structures of $[Ru_3(\mu\text{-}H)_3(CO)_9(\mu_3\text{-}Bi)]$, $[Ru_3(CO)_9(\mu_3\text{-}Bi)_2]$, and $[Ru_4(CO)_{12}(\mu_4\text{-}Bi)_2]$ †

**Caroline M. Hay, Brian F. G. Johnson, Jack Lewis,* Paul R. Raithby, and Alan J. Whitton**
*University Chemical Laboratory, Lensfield Road, Cambridge CB2 1EW*

The inclusion of naked bismuth atoms into carbonyl cluster compounds of ruthenium has been achieved with the use of bismuth(III) nitrate pentahydrate, $Bi(NO_3)_3 \cdot 5H_2O$, as the bismuth containing reagent. We report the high-yield synthesis of $[Ru_3(\mu\text{-}H)_3(CO)_9(\mu_3\text{-}Bi)]$ (**1**) from the reaction of $Bi(NO_3)_3 \cdot 5H_2O$ with $[NBu_4][Ru_4H_3(CO)_{12}]$, the preparation of (**1**) and $[Ru_3(CO)_9(\mu_3\text{-}Bi)_2]$ (**2**) from $Bi(NO_3)_3 \cdot 5H_2O$ and $Na[Ru_3H(CO)_{11}]$, and the preparation of $[Ru_4(CO)_{12}(\mu_4\text{-}Bi)_2]$ (**3**) from $Bi(NO_3)_3 \cdot 5H_2O$ and $[Ru_3(CO)_{12}]$ in KOH–MeOH solution. The determination of the *X*-ray crystal structures of (**1**), (**2**), and (**3**) show that (**1**) has a slightly distorted tetrahedral heavy-metal framework with three hydrides, each bridging a Ru–Ru edge, that (**2**) has a trigonal-bipyramidal structure with the $Ru_3$ ring capped above and below by $\mu_3$-Bi atoms, and that (**3**) has a square-bipyramidal metal framework with the Ru atoms defining the equatorial square plane and the Bi atoms symmetrically $\mu_4$-capping at the axial positions.

The synthesis and chemistry of transition metal clusters containing main group elements is a rapidly expanding field.[1] The introduction of a *p*-block element into the cluster framework has two purposes: (*i*) to polarise bonding within the cluster core leading to different reaction chemistry to that observed for homometal systems and (*ii*) to act as an inert centre stabilising the cluster core towards the conditions of temperature and pressure required for catalytic reactions.

Transition metal clusters containing bismuth are of particular interest because of the relevance of these systems to mixed bismuth–transition metal oxide oxidation catalysts.[2] Also, bismuth being the heaviest stable element in the Periodic Table, can be expected to display some unique properties based on its large size. Prior to 1983, very few mixed transition metal–bismuth clusters had been characterised and these had generally been formed by anion exchange on $BiCl_3$ with small transition metal carbonyl anions, $[W_2(CO)_{10}]^{2-}$,[3] $[Co(CO)_4]^-$,[4] $[Ir(CO)_4]^-$,[5] and $[Mn(CO)_5]^-$.[6] However, recently in an elegant series of experiments, Whitmire *et al.*[7] have reinvestigated earlier reports by Hieber *et al.*,[8] of mixed bismuth–iron clusters from the reaction of mononuclear iron carbonyls with sodium bismuthate ($NaBiO_3$). The range of clusters produced in this work has prompted us to apply similar synthetic techniques in the investigation of the chemistry of the heavier Group 8 metals, Os and Ru, with various inorganic bismuth reagents. Here we report the synthesis and structures of a number of mixed bismuth–ruthenium clusters from the reactions of various ruthenium carbonyl clusters with $NaBiO_3$ and with the previously unused bismuth reagent, $Bi(NO_3)_3 \cdot 5H_2O$. Parts of this work have been previously communicated.[9]

## Results and Discussion

The reaction of $NaBiO_3$ with the ruthenium carbonyl clusters $[Ru_3(CO)_{12}]$ or $[Ru_3H(CO)_{11}]^-$, followed by treatment of the reaction mixture with HCl(g) affords after t.l.c., low (2—10%) yields of $[Ru_3(\mu\text{-}H)_3(CO)_9(\mu_3\text{-}Bi)]$ (**1**). No other neutral clusters have been isolated by this route although considerable amounts of unstable anionic products were obtained. It was felt that $NaBiO_3$ was too reactive for the ruthenium carbonyl system and an investigation into the use of other inorganic bismuth containing species was therefore undertaken. The reaction of varying ratios of $Na[Ru_3H(CO)_{11}]$ with $Bi(NO_3)_3 \cdot 5H_2O$ in MeOH at room temperature produces, after t.l.c., higher yields of (**1**), and also the previously unknown cluster $[Ru_3(CO)_9(\mu_3\text{-}Bi)_2]$ (**2**). In these reactions the use of greater than one mole equivalent of bismuth reagent severely decreases the yield of neutral clusters and again gives a number of highly unstable anionic products.

The addition of $Bi(NO_3)_3 \cdot 5H_2O$ to $[Ru_3(CO)_{12}]$ in KOH–MeOH solution at −78 °C affords, on warming to room temperature, a brown solution. Decomposition of this solution during t.l.c. gives the green cluster $[Ru_4(CO)_{12}(\mu_4\text{-}Bi)_2]$ (**3**) in *ca.* 14% yield based on Ru. The carbonyl stretching bands of (**3**) are not observed in the i.r. spectrum of the reaction mixture, but are seen after the decomposition of the unknown intermediate compound as the t.l.c. progresses. Compound (**3**) has not been observed as a product of other preparative routes.

A novel reaction occurs when $[NBu_4][Ru_4H_3(CO)_{12}]$ is treated with one mole equivalent of $Bi(NO_3)_3 \cdot 5H_2O$ at room temperature in MeOH resulting in the cleavage of a '$Ru(CO)_3$' unit to produce (**1**) in good yield (60—70%) from $[Ru_4H_4(CO)_{12}]$.

The cluster (**1**) can be crystallised from hexane solution as orange, air-stable crystals. I.r., $^1H$ n.m.r., mass spectroscopic data, and microanalytical data are presented in Table 1. The i.r. spectrum in the carbonyl stretching region is consistent with observed spectra in other symmetrical $[M_3(\mu_3\text{-}E)(CO)_9]$ species (E = CCl, CBr, CPh, COMe, or CH; M = Ru or Os).[10] Microanalytical and mass spectral data confirm the formula, and the $^1H$ n.m.r. singlet at −17.73 p.p.m., in the room temperature spectrum, is consistent with the interpretation that in solution all three hydrides are bridging equivalent Ru–Ru edges. The mass spectrum of (**1**) shows a strong isotopic envelope centred at *m/e* 769 corresponding to the $[Ru_3H_3(CO)_9Bi]^+$ ion. The fragmentation envelopes corresponding to the ions $[Ru_3H_{3-n}(CO)_{9-m}Bi]^+$ ($n$ = 0—3, $m$ = 0—9) are observed, with an intense envelope centred at *m/e* 514 corresponding to the $[Ru_3Bi]^+$ heavy-metal framework.

In order to confirm the molecular geometry of $[Ru_3(\mu\text{-}H)_3\text{-}$

---

† $\mu_3$-Bismuthido-tri-$\mu$-hydrido-*triangulo*-tris(tricarbonylruthenium), di-$\mu_3$-bismuthido-*triangulo*-tris(tricarbonylruthenium), and di-$\mu_4$-bismuthido-tetrakis(tricarbonylruthenium) respectively.

*Supplementary data available:* see Instructions for Authors, *J. Chem. Soc., Dalton Trans.*, 1988, Issue 1, pp. xvii—xx.

Table 1. Physical data

| | | | | Analysis (%) | | | |
|---|---|---|---|---|---|---|---|
| | | | | Found | | Calc. | |
| Compound | I.r. spectra (hexane) ($cm^{-1}$)* | $^1H$ N.m.r. (p.p.m.) | Mass spectrum | C | H | C | H |
| (1) $[Ru_3(\mu\text{-}H)_3(CO)_9(\mu_3\text{-}Bi)]$ | 2 099vw, 2 070vs, 2 027vs, 2 014m, 1 987vw, 1 978vw | −17.73 | 769 | 14.20 | 0.40 | 14.10 | 0.40 |
| (2) $[Ru_3(CO)_9(\mu_3\text{-}Bi)_2]$ | 2 036s, 1 990w | — | 975 | 11.30 | — | 11.10 | — |
| (3) $[Ru_4(CO)_{12}(\mu_4\text{-}Bi)_2]$ | 2 046s, 2 001w | — | 1 160 | 12.85 | 0.40 | 12.45 | 0.0 |

* w = Weak, m = medium, s = strong, v = very.

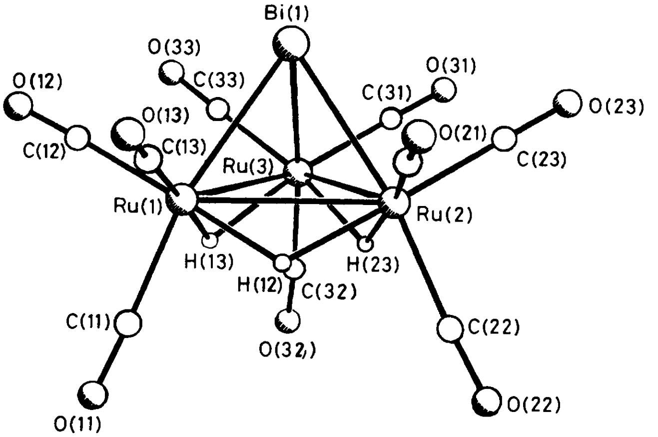

**Figure 1.** The molecular structure of $[Ru_3(\mu\text{-}H)_3(CO)_9(\mu_3\text{-}Bi)]$ (1) showing the atom numbering scheme

Table 2. Selected bond lengths (Å) and angles (°) in $[Ru_3(\mu\text{-}H)_3(CO)_9(\mu_3\text{-}Bi)]$ (1)

| | | | |
|---|---|---|---|
| Bi(1)–Ru(1) | 2.756(1) | Bi(1)–Ru(2) | 2.755(1) |
| Bi(1)–Ru(3) | 2.763(1) | Ru(1)–Ru(2) | 2.972(1) |
| Ru(1)–Ru(3) | 2.973(1) | Ru(2)–Ru(3) | 2.962(1) |
| Ru–$C_{eq}$ (av.) | 1.93(1) | Ru–$C_{ax}$ (av.) | 1.90(1) |
| C–O (av.) | 1.13(1) | Ru(1)–H(12) | 1.72(7) |
| Ru(2)–H(12) | 1.79(7) | Ru(2)–H(23) | 1.79(7) |
| Ru(3)–H(23) | 1.76(7) | Ru(3)–H(13) | 1.88(7) |
| Ru(1)–H(13) | 1.76(7) | | |
| Ru(1)–Bi(1)–Ru(2) | 65.3(1) | Ru(1)–Bi(1)–Ru(3) | 65.3(1) |
| Ru(2)–Bi(1)–Ru(3) | 64.9(1) | Ru(1)–Ru(2)–Ru(3) | 60.1(1) |
| Ru(2)–Ru(3)–Ru(1) | 60.1(1) | Ru(3)–Ru(1)–Ru(2) | 59.8(1) |
| Ru(1)–H(12)–Ru(2) | 115(4) | Ru(1)–H(13)–Ru(3) | 109(5) |
| Ru(2)–H(23)–Ru(3) | 115(4) | Ru–Ru–C | 93(1)–99(1) |
| H(12)–Ru(1)–C(12) | 175.4(28) | H(12)–Ru(2)–C(23) | 175.3(26) |
| H(13)–Ru(1)–C(13) | 175.7(26) | H(13)–Ru(3)–C(31) | 173.1(20) |
| H(23)–Ru(2)–C(21) | 170.0(19) | H(23)–Ru(3)–C(33) | 171.4(21) |
| Bi(1)–Ru(1)–C(11) | 167.5(2) | Bi(1)–Ru(2)–C(22) | 169.5(4) |
| Bi(1)–Ru(3)–C(32) | 166.9(3) | Ru–C–O (av.) | 177.4(9) |

$(CO)_9(\mu_3\text{-}Bi)]$ (1), an *X*-ray crystallographic study has been carried out. It was found that (1) and the osmium analogue[9] are isostructural with the previously reported iron cluster, $[Fe_3(\mu\text{-}H)_3(CO)_9(\mu_3\text{-}Bi)]$.[7e] The molecular structure of (1) is given in Figure 1, and selected bond lengths and angles in Table 2.

The molecule consists of a trigonal pyramidal $BiRu_3$ core, the ruthenium atoms defining a slightly distorted basal equilateral triangle with the bismuth atom sitting 2.16 Å above this plane. The three hydride ligands were directly located in the crystallographic study, each bridging a Ru–Ru edge and *ca.* 0.87 Å on the opposite side of the $Ru_3$ triangle to the capping bismuth atom. The hydride ligands exhibit bond lengths and angles consistent with those observed in other systems.[11–13] Each ruthenium atom is also associated with three terminal carbonyl ligands, two equatorial, which are *ca. trans* to the Ru–H vectors (C–Ru–H 170—176°), and one axial on the opposite side of the $Ru_3$ ring to the bismuth atom. These show the usual trend[11–14] of slightly shorter Ru–$C_{eq}$ distances (1.90 Å av.) than their axial counterparts (1.93 Å av.). The C–O bond lengths show no significant difference between axial and equatorial. All Ru–C–O bond angles approach linearity.

The average Ru–Ru distance of 2.967 Å is significantly longer than the corresponding distance of 2.885 Å in the binary carbonyl $[Ru_3(CO)_{12}]$,[14] and longer than the hydride-bridged edges observed in $Ru_3$ clusters capped by smaller bridgehead atoms.[11,12] Two factors contribute to this bond elongation. These are the presence of bridging hydrides and the steric bulk of the bismuth atom.

The effect of the hydride ion is illustrated by the complexes $[Ru_3H_2(CO)_9(\mu_3\text{-}S)]$[12] and $[Ru_3H_2(CO)_9(\mu_3\text{-}PPh)]$[13] where the bond lengths of the non-bridged edges are respectively 0.12 and 0.09 Å shorter than the distances in the hydride-bridged edges. A useful comparison can also be made within the molecule $[Ru_3(CO)_9(\mu\text{-}H)\{\mu\text{-}Au(PPhMe_2)\}(\mu_3\text{-}PPh)]$,[15] where two of the Ru–Ru bonds are bridged by two electronically similar but sterically different groups. The gold bridged Ru–Ru distance of length 3.002(5) Å, the hydride-bridged distance [2.972(5) Å], and the non-bridged distance [2.866(5) Å] provide a useful comparison for the electronic extension of bonds by hydride ligands and also for the further bond elongation caused by steric interaction.

The bond lengthening effect of the bismuth atom can be observed in the comparison of Ru–Ru bond lengths of (1) and $[Ru_3H_3(CO)_9(\mu_3\text{-}CCl)]$ (2.85 Å).[11] It is also observed that a $\mu_3$-capping main group atom normally causes a decrease in Ru–Ru bond length, but the steric bulk of the bismuth atom more than counterbalances this effect. This effect is illustrated in the iron system where the Fe–Fe distance of 2.628(2) Å in $[Fe_3(CO)_9(\mu_3\text{-}As)_2]$[16] is shorter than the unbridged distance of 2.680(2) Å in $[Fe_3(CO)_{12}]$,[17] which is itself shorter than the Fe–Fe separation of 2.735(5) Å found in $[Fe_3(CO)_9(\mu_3\text{-}Bi)_2]$.[7b]

A further effect of the large steric bulk of the bismuth atom is the acute Ru–Bi–Ru angle found [65.1(2)°]. In other $Ru_3$ clusters with smaller bridgehead atoms, the smaller bonding radius and hence closer approach to the $Ru_3$ ring gives a less acute angle, 88(1)° for $[Ru_3(\mu\text{-}H)_3(CO)_9(\mu_3\text{-}CCl)]$[11] or 73(2)° for a hydride-bridged Ru–Ru edge in $[Ru_3(\mu\text{-}H)_2(CO)_9(\mu_3\text{-}S)]$.[12]

Dark red crystals of $[Ru_3(CO)_9(\mu_3\text{-}Bi)_2]$ (2) were obtained from hexane–white spirit solution at −30 °C over a period of months. The two band i.r. spectrum in hexane solution is similar to that found for the known clusters $[Fe_3(CO)_9(\mu_3\text{-}E)_2]$ (E = As[16] or Bi[7b]). Hence, by analogy, it was assumed that the

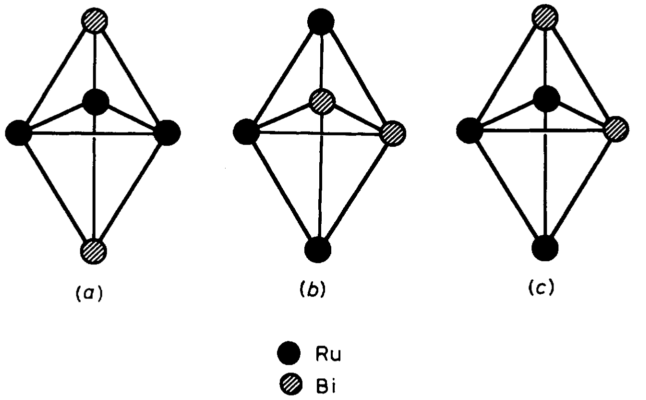

Figure 2. Possible structural isomers of $[Ru_3(CO)_9(\mu_3\text{-}Bi)_2]$ (**2**)

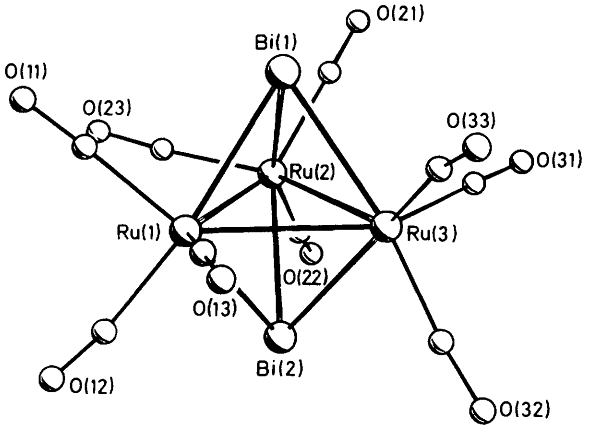

Figure 3. The structure of one of the independent molecules of $[Ru_3(CO)_9(\mu_3\text{-}Bi)_2]$ (**2**) showing the atom numbering scheme

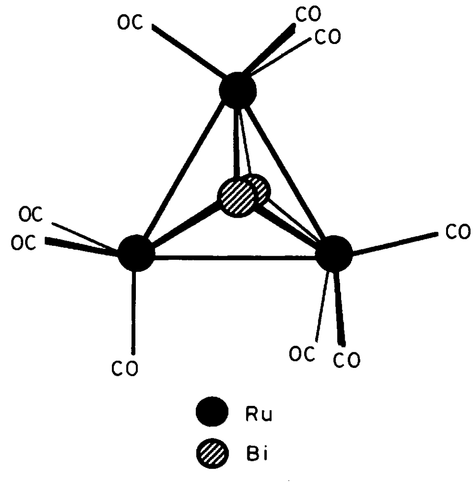

Figure 4. The orientation of the equatorial carbonyls in (**2**)

metal framework will be trigonal bipyramidal, with the bismuth atoms occupying both the axial sites [Figure 2(*a*)]. This is only one of three possible isomeric structures (Figure 2) which are indistinguishable by electron counting procedures, however the i.r. spectrum of an alternative, lower symmetry skeletal framework might be expected to exhibit a larger number of carbonyl bands than is observed. The mass spectrum of (**2**) exhibits the strong isotopic envelope of the $[Ru_3(CO)_9Bi_2]^+$ ion centred at *m*/*e* 975 followed by nine losses of carbonyl ligands (*m*/*e* 28) giving the metal skeleton envelope centred at *m*/*e* 723.

**Table 3.** Selected bond lengths (Å) and angles (°) in $[Ru_3(CO)_9(\mu_3\text{-}Bi)_2]$ (**2**)

| | | | |
|---|---|---|---|
| Molecule 1 | | | |
| Bi(1)–Ru(1) | 2.753(2) | Bi(2)–Ru(1) | 2.741(2) |
| Bi(1)–Ru(2) | 2.767(2) | Bi(2)–Ru(2) | 2.725(2) |
| Bi(1)–Ru(3) | 2.752(2) | Bi(2)–Ru(3) | 2.738(2) |
| Ru(1)–Ru(2) | 2.940(2) | Ru(2)–Ru(3) | 2.934(2) |
| Ru(1)–Ru(3) | 2.947(3) | Ru(1)–C(11) | 1.925(33) |
| Ru(1)–C(12) | 1.960(30) | Ru(1)–C(13) | 1.821(22) |
| Ru(2)–C(21) | 1.984(34) | Ru(2)–C(22) | 1.921(29) |
| Ru(2)–C(23) | 1.892(37) | Ru(3)–C(31) | 1.937(34) |
| Ru(3)–C(32) | 1.900(34) | Ru(3)–C(33) | 1.994(32) |
| C–O (av.) | 1.12(3) | Bi(1) ··· Bi(2) | 4.317(2) |
| Molecule 2 | | | |
| Bi(3)–Ru(4) | 2.746(2) | Bi(4)–Ru(4) | 2.781(2) |
| Bi(3)–Ru(5) | 2.747(2) | Bi(4)–Ru(5) | 2.748(2) |
| Bi(3)–Ru(6) | 2.735(2) | Bi(4)–Ru(6) | 2.746(2) |
| Ru(4)–Ru(5) | 2.894(3) | Ru(5)–Ru(6) | 2.958(3) |
| Ru(4)–Ru(6) | 2.938(2) | Ru(4)–C(41) | 1.893(30) |
| Ru(4)–C(42) | 1.928(29) | Ru(4)–C(43) | 1.859(28) |
| Ru(5)–C(51) | 1.910(26) | Ru(5)–C(52) | 1.942(37) |
| Ru(5)–C(53) | 1.885(23) | Ru(6)–C(61) | 1.855(31) |
| Ru(6)–C(62) | 1.884(21) | Ru(6)–C(63) | 1.944(31) |
| C–O (av.) | 1.14(2) | Bi(3) ··· Bi(4) | 4.336(2) |
| Bi(2) ··· Bi(4) | 4.195(2) | Bi(3) ··· Bi(3′) | 4.143(2) |
| Molecule 1 | | | |
| Bi(1)–Ru(1)–Bi(2) | 103.6(1) | Ru(1)–Ru(2)–Ru(3) | 60.2(1) |
| Bi(1)–Ru(2)–Bi(2) | 103.6(1) | Ru(2)–Ru(3)–Ru(1) | 60.0(1) |
| Bi(1)–Ru(3)–Bi(2) | 103.7(1) | Ru(3)–Ru(1)–Ru(2) | 59.8(1) |
| Ru(1)–Bi(1)–Ru(2) | 64.4(1) | Ru(1)–Bi(2)–Ru(2) | 65.1(1) |
| Ru(2)–Bi(1)–Ru(3) | 64.2(1) | Ru(2)–Bi(2)–Ru(3) | 65.0(1) |
| Ru(1)–Bi(1)–Ru(3) | 64.7(1) | Ru(1)–Bi(2)–Ru(3) | 65.1(1) |
| Molecule 2 | | | |
| Bi(3)–Ru(4)–Bi(4) | 103.4(1) | Ru(4)–Ru(5)–Ru(6) | 60.3(1) |
| Bi(3)–Ru(5)–Bi(4) | 104.2(1) | Ru(5)–Ru(6)–Ru(4) | 58.8(1) |
| Bi(3)–Ru(6)–Bi(4) | 104.6(1) | Ru(6)–Ru(4)–Ru(5) | 60.9(1) |
| Ru(4)–Bi(3)–Ru(5) | 63.6(1) | Ru(4)–Bi(4)–Ru(5) | 63.1(1) |
| Ru(5)–Bi(3)–Ru(4) | 65.3(1) | Ru(5)–Bi(4)–Ru(6) | 64.2(1) |
| Ru(4)–Bi(3)–Ru(6) | 64.8(1) | Ru(4)–Bi(4)–Ru(6) | 65.1(1) |

In order to elucidate the molecular structure of (**2**), a single-crystal *X*-ray study was carried out. Complex (**2**) has two independent but structurally equivalent molecules per asymmetric unit. The molecular structure of one of these is given in Figure 3, and selected bond lengths and angles in Table 3. The molecule consists of an equilateral triangle of Ru atoms capped on both sides by $\mu_3$-bridging Bi atoms. The carbonyl arrangement is similar to that found in the solid-state structures of $[Fe_3(CO)_9(\mu_3\text{-}E)_2]$ (E = As[16] or Bi[7b]) with one equatorial and two axial carbonyls per metal atom and with the equatorial ligands all orientated the same way around the $Ru_3$ plane (Figure 4). This arrangement differs from that found in the Os analogue.[18] The Ru–Ru distances in (**2**) (2.940 Å av.) are slightly shorter than observed in (**1**) (2.970 Å av.). This result is consistent with the analogous iron clusters where the Fe–Fe distance in $[Fe_3(\mu_3\text{-}H)_3(CO)_9(\mu_3\text{-}Bi)]$[7e] is slightly longer than that in $[Fe_3(CO)_9(\mu_3\text{-}Bi)_2]$.[7b] This suggests that the bond lengthening effect of a $\mu_3$-capping Bi is less than that of a $\mu$-bridging hydride ligand. The Bi–Ru distances in (**2**) (2.746 Å av.) are similar to those in (**1**) (2.759 Å av.) and the Ru–Bi–Ru angles are comparable with those in (**1**). Some Ru–C–O angles show

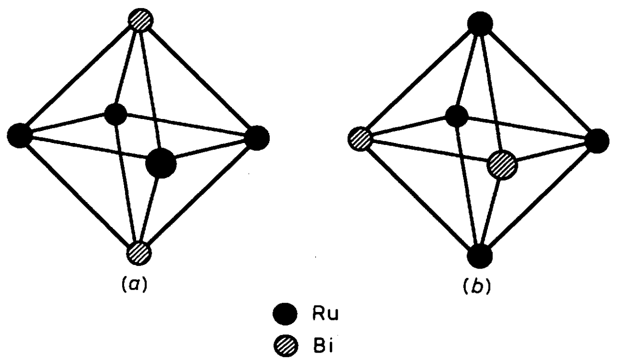

Figure 5. The two possible core geometries for $[Ru_4(CO)_{12}(\mu_4\text{-}Bi)_2]$ (3)

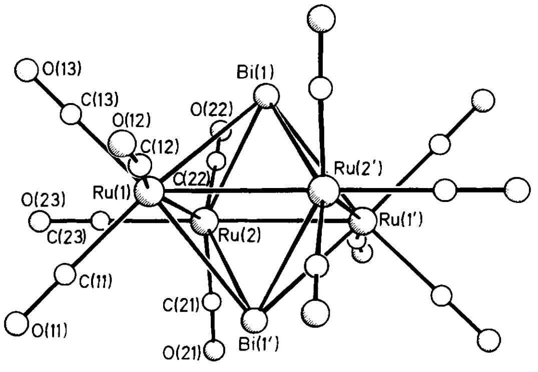

Figure 6. The molecular structure of $[Ru_4(CO)_{12}(\mu_4\text{-}Bi)_2]$ (3) showing the atom numbering scheme

slight deviations from linearity but this does not appear to be due to any intramolecular interactions. Cluster (2) is to our knowledge the first example of a closed $Ru_3$ triangle capped by two equivalent $\mu_3$-capping groups.

The cluster $[Ru_4(CO)_{12}(\mu_4\text{-}Bi)_2]$ (3) can be isolated as dark red needles from a green toluene solution. The two band i.r. spectrum is indicative of a symmetric structure in solution. The mass spectrum of (3) shows the parent isotopic envelope at *m/e* 1 160 corresponding to the $[Ru_4(CO)_{12}Bi_2]^+$ ion, followed by the envelopes at intervals of *m/e* 28 of the $[Ru_4(CO)_{12-n}Bi_2]^+$ ions ($n$ = 0—12) resulting in the heavy-metal skeleton envelope at *m/e* 824.

The effective atomic number rule (counting the bismuths as core atoms) predict that there will be 12 metal–metal contacts (Ru–Ru, Ru–Bi, or Bi–Bi) in this molecule which allows two possible core geometries (Figure 5). To distinguish between these, an *X*-ray crystal structure of (3) was carried out. Its molecular structure is given in Figure 6 with selected bond lengths and angles in Table 4. The molecule, which sits on a crystallographic centre of symmetry, consists of a square bipyramidal shaped metal skeleton with the four ruthenium atoms defining the equatorial square plane and the two $\mu_4$-Bi atoms symmetrically positioned at the apices of the polyhedron. The carbonyl arrangement in (3) is similar to that observed in (2) with the four equatorial ligands orientated the same way around the plane, and also similar, although slightly distorted by the $P(OMe)_3$ group, to the ligand arrangement in $[Fe_4(CO)_{11}(\mu_4\text{-}PPh)_2\{P(OMe)_3\}]$.[19] The Ru–C–O angles show no significant deviations from linearity.

The effect of the steric bulk of the bismuth atoms is shown by the Ru–Ru bond distance of 2.904(1) Å which is longer than non-bridged Ru–Ru distances found in the isoelectronic complex $[Ru_4(\mu_4\text{-}PPh)_2(CO)_{11}]$ (2.868 Å av.)[20] or $[Ru_4(CO)_7(\mu\text{-}CO)_2(PMe_2Ph)_2(\mu_4\text{-}S)]$ (2.79 Å av.).[21] The

Table 4. Selected bond lengths (Å) and angles (°) of $[Ru_4(CO)_{12}(\mu_4\text{-}Bi)_2]$ (3)

| | | | |
|---|---|---|---|
| Bi(1)–Ru(1) | 2.834(1) | Bi(1)–Ru(2) | 2.833(1) |
| Bi(1)–Ru(1') | 2.839(1) | Bi(1)–Ru(2') | 2.839(1) |
| Ru(1)–Ru(2) | 2.904(1) | Ru(1)–Ru(2') | 2.910(1) |
| Ru(1)–C(11) | 1.913(15) | Ru(1)–C(12) | 1.879(14) |
| Ru(1)–C(13) | 1.932(14) | Ru(2)–C(21) | 1.913(16) |
| Ru(2)–C(22) | 1.879(17) | Ru(2)–C(23) | 1.891(12) |
| C–O (av.) | 1.13(2) | | |
| Ru(1)–Bi(1)–Ru(2) | 61.6(1) | Ru(1)–Bi(1)–Ru(1') | 92.9(1) |
| Ru(1)–Ru(2)–Ru(1') | 90.0(1) | Ru(2)–Ru(1)–Ru(2') | 90.0(1) |
| Bi(1)–Ru(1)–Bi(1') | 87.1(1) | Bi(1)–Ru(2)–Bi(1') | 87.1(1) |
| C(12)–Ru(1)–Ru(2) | 164.3(4) | C(23)–Ru(2)–Ru(1') | 164.0(5) |
| Ru(1)–C(11)–O(11) | 179.2(13) | Ru(1)–C(12)–O(12) | 170.9(13) |
| Ru(1)–C(13)–O(13) | 178.4(14) | Ru(2)–C(21)–O(21) | 177.0(4) |
| Ru(2)–C(22)–O(22) | 177.4(15) | Ru(2)–C(23)–O(23) | 175.0(12) |

Bi–Ru bond lengths (2.834 Å) in (3) are longer than the corresponding lengths in (1) and (2), which is consistent with the bismuth interacting with four Ru atoms rather than three. The acute Ru–Bi–Ru angle generated [61.6(1)°] is, to our knowledge, the most acute Ru–E–Ru angle yet reported.

An osmium cluster of formula $[Os_4(CO)_{12}Bi_2]$ has been prepared and structurally characterised.[9] This cluster has the isomeric core geometry of the $E_2M_4$ polyhedron with the two bismuths bonded together over an $Os_4$ butterfly [Figure 5(*b*)].

A parallel can be drawn between bismuth- and sulphido-$M_4E_2$ (M = Ru or Os) clusters that have been synthesised. In the case of Ru, the isoelectronic $Ru_4(\mu_4\text{-}E)_2$ (E = S or Bi) units have the same structural pattern with the heteroatoms capping a $Ru_4$ square plane, whereas the structures of the clusters $[Os_4(CO)_{12}(\mu_4\text{-}Bi)_2]$ and $[Os_4(CO)_{12}(\mu_3\text{-}S)_2]$,[22] are based on an $Os_4$ butterfly structure. This may suggest some thermodynamic preference in the Os system for the formation of metal–metal bonding interactions as opposed to metal–ligand interactions.

## Experimental

All reactions were performed under dry nitrogen using standard Schlenk techniques. All solvents were freshly distilled from usual drying agents prior to use. The neutral products are sufficiently air stable to be separated by t.l.c. on silica plates. Starting materials $[Ru_3(CO)_{12}]$[23] and $[Ru_4H_4(CO)_{12}]$[24] were prepared by the standard literature preparations. Other reagents were used as supplied. I.r. spectra were obtained using a Perkin-Elmer 1700 Fourier-transform i.r. spectrometer, n.m.r. spectra on a Bruker WM250 spectrometer, and mass spectra on a Kratos MS12.

(*a*) *Preparations of* $[Ru_3(\mu\text{-}H)_3(CO)_9(\mu_3\text{-}Bi)]$ (1).—(*i*) The reaction of $[Ru_4H_4(CO)_{12}]$ (52 mg, 0.070 mmol) with KOH–EtOH (2.2 cm$^3$ of a 0.033 mmol cm$^{-3}$ solution) at 55 °C for *ca.* 1 h followed by the addition of $[NBu_4]Br$ (23 mg, 0.07 mmol) gave a red solution of $[NBu_4][Ru_4H_3(CO)_{12}]$.[25] Purification by the removal of the ethanol *in vacuo* and extraction with filtering into dichloromethane (10 cm$^3$ then two aliquots of 3 cm$^3$ each) yielded sufficiently pure $[NBu_4][Ru_4H_3(CO)_{12}]$ for further reaction. The $CH_2Cl_2$ was removed *in vacuo* and the residue dissolved in MeOH (10 cm$^3$). To this solution $Bi(NO_3)_3\cdot5H_2O$ [31 mg, 0.063 mmol in MeOH (4 cm$^3$)] was added slowly (20 min) with stirring. The product solution was reduced in volume and purified by t.l.c. (hexane as eluant). The fastest moving band was (1). Yield: 36 mg, 0.047 mmol, 68% from $[Ru_4H_4(CO)_{12}]$.

**Table 5.** Crystal data, data collection, and processing parameters* for (**1**), (**2**), and (**3**)

| Compound | (**1**) | (**2**) | (**3**) |
|---|---|---|---|
| Formula | $C_9H_3BiO_9Ru_3$ | $C_9Bi_2O_9Ru_3$ | $C_{12}Bi_2O_{12}Ru_4$ |
| *M* | 767.3 | 973.26 | 1 157.96 |
| Crystal system | Triclinic | Triclinic | Monoclinic |
| $a$/Å | 8.253(1) | 9.137(3) | 11.516(3) |
| $b$/Å | 9.300(1) | 9.350(3) | 7.420(3) |
| $c$/Å | 12.568(1) | 22.943(10) | 12.603(3) |
| $\alpha$/° | 88.03(3) | 86.0(3) | — |
| $\beta$/° | 71.73(2) | 88.2(3) | 91.12(3) |
| $\gamma$/° | 68.96(1) | 69.9(2) | — |
| $U$/Å$^3$ | 851.60 | 1 724.8 | 1 076.62 |
| Space group | $P\bar{1}$ (no. 2) | $P\bar{1}$ (no. 2) | $P2_1/n$ (alternate setting of $P2_1/c$, no. 14) |
| $D_c$/g cm$^{-3}$ | 2.99 | 3.74 | 3.57 |
| $Z$ | 2 | 4 | 2 |
| Crystal habit | Plates | Plates | Needles |
| Colour | Orange | Dark red | Dark red |
| Dimensions/mm | 0.019 × 0.28 × 0.31 | 0.02 × 0.24 × 0.36 | 0.38 × 0.19 × 0.19 |
| $F$(000) | 688 | 1 696 | 1 020 |
| $\mu$(Mo-$K_\alpha$)/cm$^{-1}$ | 128.45 | 228.16 | 189.59 |
| No. of reflections used to determine cell | 50 | 54 | 48 |
| 2θ range/° | 25—30 | 18—25 | 18—25 |
| Collection mode | ω/θ | ω/θ | ω/θ |
| Step width (ω) | 0.05 | 0.05 | 0.04 |
| No. steps/scan | 24 | 24 | 24 |
| Scan time per step/s | 0.05—2.0 | 0.75—3.0 | 0.5—2.0 |
| 2θ limits/° | 5—50 | 5—45 | 5—50 |
| Index limits | $-h \pm k \pm l$ | $-h \pm k \pm l$ | $\pm h + k \pm l$ |
| No. of reflections | 3 213 | 4 837 | 4 304 |
| Unique | 2 986 | 4 499 | 1 981 |
| Merging *R* | 0.018 | 0.022 | 0.030 |
| No. reflections with $F > 4\sigma(F)$ | 2 791 | 3 217 | 1 552 |
| Absorption correction | Numerical | Numerical | Azimuthal scan |
| Transmission factors max., min. | 0.613, 0.034 | 0.646, 0.037 | 0.038, 0.007 |

* All data were collected on a Stoe-Siemens four-circle diffractometer using graphite-monochromated Mo-$K_\alpha$ radiation. During data collection, three reflections were monitored regularly and in each case no significant fluctuations in intensity were observed.

**Table 6.** Atomic co-ordinates (× $10^4$) for $[Ru_3(\mu\text{-}H)_3(CO)_9(\mu_3\text{-}Bi)]$ (**1**)

| Atom | *x* | *y* | *z* |
|---|---|---|---|
| Bi(1) | 5 072(1) | 2 153(1) | 5 993(1) |
| Ru(1) | 6 976(1) | 1 213(1) | 7 501(1) |
| Ru(2) | 2 904(1) | 2 420(1) | 8 203(1) |
| Ru(3) | 4 903(1) | 4 523(1) | 7 340(1) |
| C(11) | 7 871(11) | 926(9) | 8 765(8) |
| O(11) | 8 464(10) | 766(9) | 9 481(7) |
| C(12) | 9 206(11) | 1 094(9) | 6 379(8) |
| O(12) | 10 531(9) | 1 076(8) | 5 745(7) |
| C(13) | 7 366(11) | −885(10) | 7 124(9) |
| O(13) | 7 537(10) | −2 121(7) | 6 938(8) |
| C(21) | 2 756(11) | 476(10) | 7 919(8) |
| O(21) | 2 625(11) | −641(7) | 7 771(7) |
| C(22) | 1 716(13) | 2 714(10) | 9 816(8) |
| O(22) | 930(12) | 2 904(9) | 10 752(7) |
| C(23) | 825(11) | 3 561(10) | 7 784(9) |
| O(23) | −424(10) | 4 313(9) | 7 539(8) |
| C(31) | 2 987(11) | 6 029(9) | 6 895(7) |
| O(31) | 1 854(8) | 6 916(7) | 6 653(6) |
| C(32) | 4 934(11) | 5 820(9) | 8 511(8) |
| O(32) | 5 047(10) | 6 528(8) | 9 165(7) |
| C(33) | 6 790(11) | 4 840(9) | 6 158(7) |
| O(33) | 7 946(9) | 5 028(8) | 5 422(6) |

(*ii*) A thf (tetrahydrofuran) solution of $[Ru_3(CO)_{12}]$ (20 mg, 0.031 mmol in 10 cm$^3$) was stirred at room temperature with $NaBH_4$ (8 mg) for 30 min. The solvent was removed *in vacuo* and the red $Na[Ru_3H(CO)_{11}]$[26] extracted with $CH_2Cl_2$ and filtered through a Celite plug. The $CH_2Cl_2$ was subsequently removed and MeOH (10 cm$^3$) added followed by cooling to −78 °C in a dry ice–acetone bath. To this solution a fine suspension of $Bi(NO_3)_3{\cdot}5H_2O$ (14 mg, 0.031 mmol) in MeOH (5 cm$^3$) was slowly added (20 min) and the mixture allowed to warm to room temperature. Removal of solvent and extraction with $CH_2Cl_2$ yielded a variety of products, the main being (**1**). These can be separated by t.l.c. with hexane as eluant. Yield: 2—8 mg, 10—35%. **NB.** *Could not be successfully scaled up.*

(*iii*) A mixture of $[Ru_3(CO)_{12}]$ (20 mg, 0.031 mmol) {or $Na[Ru_3H(CO)_{11}]$ from $[Ru_3(CO)_{12}]$ (20 mg)} and $NaBiO_3$ (8 mg, 0.029 mmol) was stirred at room temperature for 1 h. The resultant very dark coloured solution was treated with HCl(g), which was bubbled through the solution for 5 s and then reduced in volume to *ca.* 5 cm$^3$ and hexane added (10 cm$^3$ then 4 aliquots of 5 cm$^3$) to extract the neutral products. These were separated by t.l.c. giving two identifiable compounds, (**1**) and $[Ru_3(CO)_{12}]$. Yield of (**1**): < 1—2 mg, < 5—10%.

(*b*) *Preparation of* $[Ru_3(CO)_9(\mu_3\text{-}Bi)_2]$ (**2**).—As in (*a*) (*ii*), but using $Bi(NO_3)_3{\cdot}5H_2O$ (30 mg, 0.62 mmol). The mixture was stirred for 4 h and the products separated by t.l.c. using hexane–$CH_2Cl_2$ (85:15%) as eluant. The very light brown Band 4 was $[Ru_3(CO)_9(\mu_3\text{-}Bi)_2]$. Yield: < 1 mg, < 5%.

(*c*) *Preparation of* $[Ru_4(CO)_{12}(\mu_4\text{-}Bi)_2]$ (**3**).—To a solution of KOH–MeOH (0.10 g in 20 cm$^3$) at −78 °C was added $[Ru_3(CO)_{12}]$ (50 mg, 0.078 mmol) and $Bi(NO_3)_3{\cdot}5H_2O$ (115 mg, 0.24 mmol). The solution was allowed to warm to room temperature giving a brown solution and stirred for 2 h, then reduced in volume and run up a silica plate with $CH_2Cl_2$ as

**Table 7.** Atomic co-ordinates ( × $10^4$) for [$Ru_3(CO)_9(\mu_3\text{-}Bi)_2$] (**2**)

| Atom | *x* | *y* | *z* |
|---|---|---|---|
| Bi(1) | 10 720(1) | 6 683(1) | 9 625(1) |
| Bi(2) | 12 031(1) | 7 128(1) | 7 823(1) |
| Ru(1) | 11 483(2) | −1 379(2) | 8 853(1) |
| Ru(2) | 13 099(2) | −4 929(2) | 8 799(1) |
| Ru(3) | 9 568(2) | −2 985(2) | 8 503(1) |
| C(11) | 12 441(39) | −1 130(32) | 9 550(12) |
| O(11) | 12 987(35) | −929(28) | 9 948(11) |
| C(12) | 12 572(31) | −373(30) | 8 355(10) |
| O(12) | 13 130(33) | 311(31) | 8 157(11) |
| C(13) | 9 471(34) | 421(30) | 8 893(13) |
| O(13) | 8 186(25) | 1 534(20) | 8 841(12) |
| C(21) | 13 067(37) | −6 722((34) | 9 305(15) |
| O(21) | 13 189(28) | −7 822(22) | 9 562(12) |
| C(22) | 14 319(29) | −6 288(28) | 8 181(15) |
| O(22) | 15 132(27) | −7 239(23) | 7 884(12) |
| C(23) | 14 944(37) | −4 845(33) | 9 115(15) |
| O(23) | 16 007(24) | −4 785(26) | 9 342(13) |
| C(31) | 9 717(32) | −5 116(34) | 8 479(16) |
| O(31) | 9 758(30) | −6 293(24) | 8 456(14) |
| C(32) | 8 557(40) | −2 155(39) | 7 758(15) |
| O(32) | 7 890(34) | −1 752(27) | 7 299(15) |
| C(33) | 7 452(39) | −1 920(43) | 8 947(15) |
| O(33) | 6 212(28) | −1 268(34) | 9 108(14) |
| Bi(3) | 8 871(1) | 3 644(1) | 5 329(1) |
| Bi(4) | 8 961(1) | 1 866(1) | 7 131(1) |
| Ru(4) | 7 397(2) | 4 647(2) | 6 388(1) |
| Ru(5) | 8 278(2) | 1 447(2) | 6 016(1) |
| Ru(6) | 10 921(2) | 2 288(2) | 6 278(1) |
| C(41) | 6 773(28) | 5 344(25) | 7 154(14) |
| O(41) | 6 282(27) | 5 962(24) | 7 596(10) |
| C(42) | 7 337(29) | 6 665(29) | 6 107(12) |
| O(42) | 7 214(27) | 7 875(21) | 5 938(10) |
| C(43) | 5 293(30) | 5 113(27) | 6 143(15) |
| O(43) | 4 002(28) | 5 362(24) | 5 981(14) |
| C(51) | 6 487(27) | 1 275(23) | 6 407(10) |
| O(51) | 5 360(19) | 1 266(21) | 6 611(9) |
| C(52) | 7 508(32) | 1 338(28) | 5 248(16) |
| O(52) | 6 985(30) | 1 183(27) | 4 819(9) |
| C(53) | 9 766(26) | −789(31) | 6 127(14) |
| O(53) | 10 677(24) | 2 135(20) | 6 168(12) |
| C(61) | 11 380(26) | 3 523(28) | 6 768(13) |
| O(61) | 11 731(27) | 4 230(25) | 7 083(11) |
| C(62) | 12 530(29) | 230(27) | 6 578(15) |
| O(62) | 13 549(24) | −1 041(20) | 6 715(12) |
| C(63) | 12 458(34) | 2 307(32) | 5 677(13) |
| O(63) | 13 396(22) | 2 339(24) | 5 368(10) |

**Table 8.** Atomic co-ordinates ( × $10^4$) for [$Ru_4(CO)_{12}(\mu_4\text{-}Bi)_2$] (**3**)

| Atom | *x* | *y* | *z* |
|---|---|---|---|
| Bi(1) | 4 871(1) | −2 538(1) | 4 598(1) |
| Ru(1) | 5 412(1) | 645(1) | 3 466(1) |
| Ru(2) | 3 269(1) | 359(2) | 4 632(1) |
| C(11) | 5 010(11) | 2 823(20) | 2 734(11) |
| O(11) | 4 789(9) | 4 094(15) | 2 304(9) |
| C(12) | 6 980(12) | 721(23) | 3 082(10) |
| O(12) | 7 870(10) | 901(24) | 2 743(9) |
| C(13) | 4 950(13) | −760(20) | 2 237(11) |
| O(13) | 4 707(10) | −1 596(18) | 1 526(8) |
| C(21) | 2 294(13) | 2 140(22) | 5 257(12) |
| O(21) | 1 691(12) | 3 156(23) | 5 590(11) |
| C(22) | 2 125(14) | −1 432(26) | 4 747(12) |
| O(22) | 1 416(13) | −2 569(21) | 4 779(12) |
| C(23) | 2 818(11) | 921(20) | 3 219(10) |
| O(23) | 2 468(9) | 1 266(17) | 2 404(9) |

eluant. During the chromatography, the brown compound was converted to the green complex (**3**) which moves closely behind the solvent front and is obtained cleanly from the t.l.c. plate. Yield: 10 mg, 14%.

*Crystal Structure Determination and Refinements.*—Suitable single crystals of the compounds were mounted on glass fibres with epoxy resin. Details of crystal data and data collection and refinement parameters are given in Table 5.

For structures (**1**) and (**3**) the unique Bi atom position was derived from a Patterson synthesis, and for structure (**2**) the four unique Bi atom positions were located by centrosymmetric direct methods. The remaining atoms, including the hydrogens in structure (**1**), were located from subsequent Fourier difference syntheses. The structures were refined to convergence by blocked full-matrix least-squares techniques with all the non-hydrogen atoms assigned anisotropic thermal parameters. Weighting schemes were applied, and analyses of the variations of the sum of $w\Delta^2$ [$\Delta = (F_o - |F_c|)$] according to $|F_o|$ and sin θ indicated that the schemes were appropriate. The final residuals were calculated on the basis $R = [\Sigma|F_o - |F_c||/\Sigma F_o]$, $R' = [\Sigma w^{\frac{1}{2}}||F_o| - |F_c||/\Sigma w^{\frac{1}{2}}F_o]$, and $w = 1/[\sigma^2(F_o) + gF_o{}^2]$ where $\sigma(F_o)$ is calculated from counting statistics. The final positional co-ordinates for all the non-hydrogen atoms in (**1**), (**2**), and (**3**) are listed in Tables 6—8 respectively. All atoms were assigned complex neutral atom scattering factors which were taken from ref. 27. Calculations were performed on the University of Cambridge IBM 3081 mainframe computer using SHELX 76.[28]

Additional material available from the Cambridge Crystallographic Data Centre comprises H-atom co-ordinates, thermal parameters, and remaining bond lengths and angles.

## Acknowledgements

We thank the S.E.R.C. for financial support, B.P. for a CASE award (to C. M. H.), and the Cambridge Commonwealth Trust, Trinity College (Cambridge) and O.R.S. for awards (to A. J. W.).

## References

1 W. A. Herrman, *Angew. Chem., Int. Ed. Engl.*, 1986, **25**, 56.

2 R. K. Grasselli and J. D. Burrington, *Adv. Catal.*, 1981, **30**, 133.

3 G. Huttner, U. Weber, and L. Zsolnai, *Z. Naturforsch., Teil B*, 1982, **37**, 707.

4 G. Etzrodt, R. Boese, and G. Schmid, *Chem. Ber.*, 1979, **112**, 2574.

5 W. Kuppa, D. Blaser, R. Boese, and G. Schmid, *Z. Naturforsch., Teil B*, 1982, **37**, 209.

6 J. M. Wallis, G. Muller, and H. Schmidbaur, *Inorg. Chem.*, 1987, **26**, 458.

7 (*a*) K. H. Whitmire, C. B. Lagrone, M. R. Churchill, J. C. Fettinger, and L. V. Biondi, *Inorg. Chem.*, 1984, **23**, 4227; (*b*) K. H. Whitmire, M. R. Churchill, and J. C. Fettinger, *J. Organomet. Chem.*, 1985, **284**, 13; (*c*) K. H. Whitmire, M. R. Churchill, and J. C. Fettinger, *J. Am. Chem. Soc.*, 1985, **107**, 1056; (*d*) K. H. Whitmire, M. R. Churchill, J. C. Fettinger, and C. B. Lagrone, *J. Organomet. Chem.*, 1986, **304**, 99; (*e*) K. H. Whitmire, M. R. Churchill, and J. C. Fettinger, *Inorg. Chem.*, 1986, **25**, 2472; (*f*) K. H. Whitmire, K. S. Raghuveer, M. R. Churchill, J. C. Fettinger, and R. F. See, *J. Am. Chem. Soc.*, 1986, **108**, 2778.

8 V. W. Hieber, J. Gruber, and F. Lux, *Z. Anorg. Allg. Chem.*, 1959, **300**, 275.

9 H. G. Ang, C. M. Hay, B. F. G. Johnson, J. Lewis, P. R. Raithby, and A. J. Whitton, *J. Organomet. Chem.*, 1987, **330**, C5.

10 J. B. Keister and T. L. Horling, *Inorg. Chem.*, 1980, **19**, 2304.

11 N. J. Zhu, C. Lecomte, P. Coppens, and J. B. Keister, *Acta Crystallogr., Sect. B*, 1982, **38**, 1286.

12 R. D. Adams and D. A. Katahira, *Organometallics*, 1982, **1**, 53.
13 F. Iwasaki, M. J. Mays, P. R. Raithby, P. L. Taylor, and P. J. Wheatley, *J. Organomet. Chem.*, 1981, **213**, 185.
14 M. R. Churchill, F. L. Hollander, and J. P. Hutchinson, *Inorg. Chem.*, 1977, **16**, 2655.
15 M. J. Mays, P. R. Raithby, P. L. Taylor, and K. Henrick, *J. Organomet. Chem.*, 1982, **224**, C45.
16 L. T. J. Delbraere, L. T. Kruczynski, and D. W. McBride, *J. Chem. Soc., Dalton Trans.*, 1973, 307.
17 F. A. Cotton and J. M. Troup, *J. Am. Chem. Soc.*, 1974, **96**, 4155.
18 C. M. Hay, B. F. G. Johnson, J. Lewis, P. R. Raithby, and A. J. Whitton, unpublished work.
19 H. Vahrenkamp and D. Wolters, *Organometallics*, 1982, **1**, 874.
20 J. S. Fields, R. J. Haines, and D. N. Smit, *J. Organomet. Chem.*, 1982, **224**, C49.
21 R. D. Adams, J. E. Babin, and M. Tasi, *Inorg. Chem.*, 1986, **25**, 4514.
22 R. D. Adams, I. T. Horvath, P. Mathur, B. E. Segmuller, and L.-W. Yang, *Organometallics*, 1983, **2**, 1078.
23 A. Mantovani and S. Cenini, *Inorg. Synth.*, 1976, **16**, 47.
24 S. A. R. Knox, J. W. Koepke, M. A. Andrews, and H. D. Kaesz, *J. Am. Chem. Soc.*, 1975, **97**, 3942.
25 J. W. Koepke, J. R. Johnson, S. A. R. Knox, and R. Bau, *Inorg. Chem.*, 1978, **17**, 1271.
26 B. F. J. Johnson, J. Lewis, P. R. Raithby, and G. Süss, *J. Chem. Soc., Dalton Trans.*, 1979, 1356.
27 'International Tables for *X*-Ray Crystallography,' Kynoch Press, Birmingham, 1975, vol. 4.
28 G. M. Sheldrick, SHELX 76, Crystal Structure Determination Package, University of Cambridge, 1976.

*Received 2nd September* 1987; *Paper* 7/1609